HHS Public Access

Author manuscript

Dev Biol. Author manuscript; available in PMC 2019 August 01.

Published in final edited form as:

Dev Biol. 2018 August 01; 440(1): 40–52. doi:10.1016/j.ydbio.2018.05.003.

ETS transcription factor Etsrp / Etv2 is required for lymphangiogenesis and directly regulates *vegfr3 / flt4* expression

Jennifer A. Davis[a,1], **Andrew L. Koenig**[b,1], **Allison Lubert**[a], **Brendan Chestnut**[b], **Fang Liu**[c], **Sharina Palencia Desai**[b], **Tamara Winkler**[a], **Karolina Pociute**[b], **Kyunghee Choi**[c,d], and **Saulius Sumanas**[b,e,*]

[a]Cancer & Blood Disease Institute, Division of Oncology, Cincinnati Children's Hospital Medical Center, Cincinnati, OH, USA

[b]Division of Developmental Biology, Cincinnati Children's Hospital Medical Center, Cincinnati, OH, USA

[c]Department of Pathology and Immunology, Washington University School of Medicine, St. Louis, MO, USA

[d]Graduate School of Biotechnology, Kyung Hee University, Yong In, South Korea

[e]Department of Pediatrics, University of Cincinnati College of Medicine, Cincinnati, OH, USA

Abstract

The molecular mechanisms initiating the formation of the lymphatic system, lymphangiogenesis, are still poorly understood. Here we have identified a novel role in lymphangiogenesis for an ETS transcription factor, Etv2/Etsrp, a known regulator of embryonic vascular development. Through the use of fully validated photoactivatable morpholinos we show that inducible Etv2 inhibition in zebrafish embryos at 1 day post-fertilization (dpf) results in significant inhibition of lymphangiogenesis, while development of blood vessels is unaffected. In Etv2-inhibited embryos and larvae, the number of lymphatic progenitors is greatly reduced, the major lymphatic vessel, the thoracic duct, is absent or severely fragmented, and lymphangiogenesis-associated marker

[*]Corresponding author. Address: Cincinnati Children's Hospital Medical Center, Division of Developmental Biology, 3333 Burnet Ave., Cincinnati, OH 45229. Tel.: (513)803-0345, Fax: (513)636-4317, Saulius.Sumanas@cchmc.org.

[1]Authors made equal contributions to this study

Competing Interests

No competing interests declared.

Author contributions

J.A.D. and A.L.K. were involved in the study design, performed the experiments, analyzed the data and wrote the manuscript, A.L. and T.W. performed experiments and analyzed the data, B.C. performed luciferase assays in zebrafish and collected the data, S.P.D. assisted with experimental setup and imaging, F.L. performed ChIP-Seq and in vitro Luciferase assays and data analysis, K.P. made the *fli1a:flt4* transgenic line, K.C. designed ChIP-Seq and Luciferase assay experiments and analyzed the data, S.S. designed and supervised the study, assisted with data analysis, and edited the manuscript.

Disclosures

The authors declare no competing financial interests.

expression, including *lyve1b*, *prox1a*, and *vegfr3/flt4*, is strongly downregulated. We also demonstrate that lymphatic progenitors in Etv2 deficient embryos fail to respond to Vegfc signaling. Chromatin immunoprecipitation and sequencing (ChIP-Seq) studies using differentiated mouse embryonic stem (ES) cells as well as luciferase reporter studies in the ES cells and in zebrafish embryos argue that Etv2 directly binds the promoter/enhancer regions of Vegfc receptor *Vegfr3/Flt4* and lymphatic marker *Lyve1*, and promotes their expression. Together these data support a model where Etv2 initiates lymphangiogenesis by directly promoting the expression of *flt4* within the posterior cardinal vein.

Keywords

ETS transcription factors; Etv2; lymphangiogenesis; lymphatics; thoracic duct; zebrafish; Vegfc; Vegfr3; Flt4; Etsrp

INTRODUCTION

The lymphatic system is of clinical interest because of its essential role in pathologic settings, such as lymphedema, vascular malformation, inflammation, and cancer metastasis. Lymphangiogenesis, the sprouting of lymphatic vessels, has been studied less than the blood vessel counterpart, angiogenesis, largely due to previous limitations in visualization. As such, molecular mechanisms that regulate lymphangiogenesis remain poorly understood (Schulte-Merker et al., 2011). Lymphatic vessels transport fluid and large molecules from interstitial spaces into blood circulation or lymph nodes while providing a home for the development and transport of lymphoid cells involved in regulating the immune system (Tammela and Alitalo, 2010). This complex vessel network is constructed of blind-ended capillaries, pre-collecting and collecting vessels. Disruption in the early development and formation of these structures or failure in function inhibits fluid drainage and immune surveillance.

While the use of the zebrafish animal model for the study of lymphatics is recent, it is firmly established in literature as effective and evolutionarily conserved (Hogan et al., 2009b; Isogai et al., 2009; Kuchler et al., 2006; Le Guen et al., 2014; Schulte-Merker et al., 2011; Yaniv et al., 2006). Zebrafish are relatively inexpensive to maintain, and embryos develop rapidly compared to other vertebrate models and allow direct visualization of developing vasculature. Thus, previous observational hurdles have been overcome by the optically clear and genetically modifiable zebrafish embryo, which provides an elegant vertebrate model for understanding embryonic lymphangiogenesis, and for investigating putative therapeutic targets for inherited and acquired vascular and lymphatic pathological conditions (Schulte-Merker et al., 2011).

Similar to mammalian embryos, zebrafish lymphangioblasts are derived from the posterior cardinal vein (PCV) and can be recognized by expression of the lymphatic-specific transcription factor *prospero-related homeobox domain 1a (prox1a)* (Koltowska et al., 2015; Nicenboim et al., 2015). During the developmental time window between 36 and 48 hpf, *prox1a*-negative endothelial cells sprout from the PCV and migrate dorsally, forming intersegmental veins as they make connections to the arterial intersegmental vessels (ISVs).

Prox1a-positive sprouts from the PCV, in contrast, do not make arterial connections, but congregate as parachordal lymphangioblasts (PLs) along the horizontal myoseptum of the zebrafish trunk (48-60 hpf) (Hogan et al., 2009b; Isogai et al., 2009; Nicenboim et al., 2015; Yaniv et al., 2006). These PLs continue migrating from 60 hpf along arterial ISVs both ventrally and dorsally, away from the myoseptum to coalesce and form the thoracic duct, which localizes ventral to the DA (4-5 dpf), the intersegmental lymphatic vessels (ISLVs), and the dorsal longitudinal lymphatic vessels (DLLVs), which together comprise the foundation of the zebrafish lymphatic system (Hogan et al., 2009a; Kuchler et al., 2006; Okuda et al., 2012; Yaniv et al., 2006).

Several signaling pathways and transcription factors have been implicated in distinct steps of lymphangiogenesis. Vascular Endothelial Growth Factor C (Vegfc) and its receptor Vegfr3/Flt4 signaling is essential in promoting *Prox1* expression, lymphatic endothelial cell (LEC) proliferation, migration, and maintenance in different vertebrate models (Hogan et al., 2009b; Karkkainen et al., 2004; Koltowska et al., 2015; Villefranc et al., 2013; Yang et al., 2012). Similar to murine *Prox1* mutants, maternal-zygotic zebrafish *prox1a* mutants show strong reduction of lymphatic progenitor cells (Koltowska et al., 2015; Wigle and Oliver, 1999). The second Prox1 homolog in zebrafish, *prox1b* does not appear to have a significant contribution to lymphangiogenesis (Koltowska et al., 2015; Tao et al., 2011). Wnt5 signaling from the endoderm has been recently implicated in initiating zebrafish *prox1a* expression and lymphangiogenesis (Nicenboim et al., 2015). In addition, the members of SOX and ETS transcription factor families are known to have critical functions in lymphangiogenesis. In mice, the expression of *Sox18* in the venous endothelium commits this cell lineage to a lymphatic fate (Francois et al., 2008). The combined activity of this transcription factor with Chicken Ovalbumin Upstream Promoter-Transcription Factor II (Coup-TFII) directs polarized expression of *Prox1* in a compartment of endothelial cells within the cardinal vein at embryonic day E9.5 (Francois et al., 2008; Karkkainen et al., 2004; Srinivasan et al., 2010). An ETS transcription factor, Ets2, has been implicated in lymphangiogenesis through induction of *Flt4* expression in collaboration with Prox1 (Yoshimatsu et al., 2011). However, it is not clear if Ets2 is required for lymphangiogenesis *in vivo*. In addition, it is currently unclear if the function of Sox18 and CoupTFII is conserved between different vertebrates (Cermenati et al., 2013; van Impel et al., 2014). Therefore, transcriptional regulation of lymphangiogenesis remains poorly understood.

Etv2 is an endothelial specific ETS transcription factor that is essential for vascular differentiation and morphogenesis in multiple vertebrates. *Etv2* knockdown and mutant zebrafish embryos fail to undergo vasculogenesis and exhibit loss of multiple vascular endothelial marker expression (Pham et al., 2007; Sumanas and Lin, 2006). Similar to zebrafish, mouse *Etv2* null mutants exhibit loss of yolk sac vasculogenesis (Ferdous et al., 2009; Lee et al., 2008). In addition to early vasculogenesis, Etv2 has a separate role in sprouting angiogenesis during ISV development, where it functions redundantly with a related ETS transcription factor Fli1b (Craig et al., 2015). However, its role in lymphatic development has not yet been investigated.

Here we show that *etv2* expression in zebrafish embryos is enriched in the PCV at 36-48 hpf, when lymphatic fated progenitors emerge from the PCV. Knockdown of Etv2 using

photoactivatable morpholinos at 24 hpf, after vasculogenesis and major axial vessel formation is complete, resulted in the inhibition of parachordal lymphangioblast formation and migration, and the suppression of the subsequent development of the thoracic duct (TD). In addition, we show a concomitant reduction of genetic markers that are associated with lymphangiogenesis including *flt4/vegfr3* when Etv2 is inhibited at 24 hpf in the developing embryo. We utilized heat shock induced overexpression of *vegfc* in Etv2 depleted embryos at 24 hpf to demonstrate that Etv2 function is required for Vegfc-induced lymphangiogenesis. ChIP-Seq analysis demonstrates that Etv2 directly binds to the promoter / enhancer regions of *Flt4* and lymphatic marker *Lyve1*. These results argue that Etv2 is a novel critical regulator of lymphatic development.

MATERIALS AND METHODS

Zebrafish strains and staging

Tg(fli1a:GFP)^{y1} (Lawson and Weinstein, 2002), *Tg(kdrl:mCherry)*^{ci5} (Proulx et al., 2010), Tg(*-2.3 etv2:GFP*)^{zf372} (Veldman and Lin, 2012), TgBAC(*etv2:EGFP*)^{ci1} (Proulx et al., 2010), and TgBAC(*prox1a:KalT4-UAS:uncTagRFP*)^{nim5} (Dunworth et al., 2014*)* (further abbreviated as *prox1a:RFP)* reporter lines, and *etv2*^{y11} mutant line (Pham et al., 2007) were used for experiments in this study. The Tg*(fli1a:flt4-2A-mCherry)*^{ci29} line was generated by the Tol2-mediated transgenesis as described below in the 'Vascular specific *etv2* and *flt4* overexpression' section. Embryos and larvae were raised at 28.5°C, or 32°C to speed up development. Embryonic staging was performed according to established criteria (Kimmel et al., 1995). Zebrafish experiments were performed under CCHMC IACUC approved protocol.

Morpholinos

We previously designed and validated the photoactivatable *etv2* morpholino (MO) (PhotoMorphs, Supernova Life Sciences) (Kohli et al., 2013). In this design, a photosensitive caging strand was hybridized to the translation-blocking *etv2* antisense MO2 (MO2, CACTGAGTCCTTATTTCACTATATC; Gene Tools, Inc.), rendering it inactive (Sumanas and Lin, 2006). UV light exposure activates MO and results in inhibition of Etv2 function at select developmental stages. PhotoMorph injection was performed as described previously (Sumanas, 2017). Briefly, the night prior to injection, the caging strand designed against *etv2* MO2 was mixed with the standard *etv2* MO2 in 1× Danieau buffer (58 mM NaCl, 0.7 mM KCl, 0.4 mM MgSO4, 0.6 mM Ca $(NO_3)_2$, 5 mM HEPES, pH 7.6) to final concentrations of 500 μM and 50 μM respectively. The mixture was denatured at 70 °C for 30 minutes and then cooled slowly overnight. After establishing injection titrations to achieve effective Etv2 knockdown without toxic or off target effects, 2.5 nl of the Photomorph MO cocktail was injected into each *Tg(fli1a:GFP; kdrl:mCherry*) and other reporter embryos at the 1-2 cell stage. 1.0 nl reduced dose was used for injections into *etv2*^{y11} embryos. All solutions and injections were handled in a dark room equipped with yellow filters on all minimal light sources. Embryos were kept in the dark until uncaging. Photoactivation was performed at key developmental stages, exposing uncovered dishes to 365 nm UV light for 30 minutes at 5-10 cm distance from light source. Embryos were swirled every 10 minutes during photoactivation.

Standard control MO (CCTCTTACCTCAGTTACAATTTATA) (Gene Tools, Inc.) which has no target in the zebrafish genome was used for a control experiment. To control for any potential off-target effect of Etv2 caging strand, the solution of the standard MO and Etv2 caging strand was used for injections, which was prepared as described above at the same concentration as for Etv2 MO (500 μM and 50 μM caging strand / MO).

In situ hybridization

Whole mount *in situ* hybridization (ISH) was performed as previously described (Jowett, 1999). DIG-labeled antisense RNA probes for *etv2, lyve1b*, and *flt4* were synthesized as previously described (Hogan et al., 2009a; Sumanas et al., 2005; Thompson et al., 1998). Prior to imaging, zebrafish embryos or larvae were dehydrated to 100% ethanol, slowly rehydrated, whole mounted in 3% methylcellulose or 0.6% low melting agarose and imaged with the AxioImager compound microscope (Carl Zeiss) equipped with a Plan-Neofluar 10×/0.3 N.A. microscope objective (Carl Zeiss) and an AxioCam Icc3 color camera (Carl Zeiss, Inc.). A series of z-slices were acquired using AxioVision 4.6 software (Carl Zeiss, Inc.) to produce extended focus projected images.

Quantification of venous intersegmental vessels and lymphangioblasts

Venous ISVs were quantified at 4 dpf in uninjected, control never photoactivated *etv2* MO, and 24 hpf photoactivated *etv2* MO larvae. The percentage of ISVs with venous connections was determined by counting the total number of ISVs arterial and venous connections over 8-9 segments (this was limited by the imaged area) and dividing the number of venous connections by the total number of ISV connections per larva. The data is presented as an average of percentage of ISVs with venous connections.

Quantification of parachordal lymphangioblasts at 52 hpf was accomplished by counting the number of parachordal lymphangioblasts in ten intersegmental spaces over the trunk of each embryo per group, which was then divided over ten segments (or somites). The data is presented as the average number of PLs per segment.

To quantify *prox1a*-positive lymphangioblasts within the PCV, *prox1a:RFP; UAS:GFP* embryos were imaged at 30-32 hpf using confocal microscopy, and GFP+ cells were quantified in the region of the axial vasculature across 9 somites of the trunk. Cells immediately adjacent to the yolk extension and in the tail were excluded from quantification as the transgene is expressed in the pronephros and tail vasculature.

Heat shock induced etv2 and vegfc overexpression

To overexpress *etv2, Tg*(*fli1a*:GFP) embryos at the 1-2 cell stage were injected with a mixture of 3 pg of *hsp70:Etv2-mCherry* overexpression construct (Veldman et al., 2013), and 50 pg of *tol2* mRNA, cultured until 24 or 48 hpf, and heat-shocked at 37°C for 30 minutes to induce the overexpression of *etv2*. Embryos or larvae were fixed at 28-30 hpf and 52-54 hpf stages for ISH analysis. To overexpress *vegfc*, *Tg(fli1a:GFP; kdrl:mCherry*) embryos were injected with a mixture of 25 pg of *Tol2-hsp70:vegfc; myl7:GFP* overexpression construct (kindly donated by Ben Hogan) and 75 pg of Tol2 mRNA. The

larvae were subjected to heat-shock at 48 hpf for 30 minutes at 37°C and were raised to 52 hpf to examine marker expression by *in situ* hybridization or by fluorescence microscopy.

Vascular specific etv2 and flt4 overexpression

For vascular specific *etv2* and *flt4* overexpression, *fli1:etv2-2A-mCherry* and *fli1:flt4-2A mCherry* constructs were generated with Gateway cloning technology (Invitrogen) using the following entry clones: *p5E-fli1ep*, *pENTR – Etv2 / Flt4* (the coding sequence of Etv2 or Flt4 was PCR amplified and subcloned into pDONR221 vector using BP recombination) and *p3E-2A-mCherry*, and the destination vector pDestTol2pA (Villefranc et al., 2007). Zebrafish Flt4 coding sequence was generated by Gene synthesis with codon optimization (Genscript). *Tg(prox1a:RFP; UAS:GFP)* or *Tg(fli1a:GFP)* embryos were injected at the 1-cell stage with either *fli1:etv2-2A-mCherry* or *fli1:flt4-2A mCherry* construct at a dose of 25pg/embryo together with 60pg/embryo of *tol2* mRNA. Embryos with vascular specific mCherry expression were selected at 24 hpf for later imaging and analysis or rearing.

Imaging

Compound Microscope: Embryos and larvae were whole mounted in 3% methylcellulose or 0.6% low melting point agarose on glass slides. Images were captured using a 10× / 0.3 NA objective on AxioImager Z1 (Zeiss, Inc.) compound microscope with Axiocam ICC3 color camera (Zeiss). Images in multiple focal planes were captured individually and combined using the Extended Focus module within Axiovision software (Zeiss, Inc.).

Confocal microscope: Embryos and larvae were whole mounted in 3% methylcellulose or 0.6% low melting point agarose on glass slides. Images were captured using a 16× / 0.8 NA or 25× / 1.1 NA water immersion objective on a Nikon A1R MP upright confocal microscope in single photon mode located in the CCHMC Confocal Imaging Core (Cincinnati Children's Hospital Medical Center). Z-stacks were captured using NIS Elements analysis and projected using Surpass view in Imaris software (Bitplane).

Time-lapse imaging: Embryos and larvae were mounted in 3% methyl cellulose or 0.6% low melting point agarose on a glass slide and placed in a 100mm Petri dish filled with water on a temperature-controlled stage-top incubator (28°C). Images were captured with a 25X water immersion objective using single photon acquisition mode on a Nikon A1R MP upright confocal microscope located in the CCHMC CIC. Z-stacks were captured using NIS elements analysis and projected using Surpass view in Imaris software (Bitplane).

Luciferase experiments

In vitro luciferase assays in 293T cells were performed as previously described (Liu et al., 2015). Briefly, Etv2 bound putative enhancer sequences (Table S1) obtained through MACS peak-calling algorithm were PCR-amplified and cloned into the pGL4.24[*luc2*P/minP] vector containing the minimal promoter and the luciferase reporter gene *luc2P*. For luciferase assays, 293T cells cultured in DMEM supplemented with 10% fetal bovine serum were plated onto 24-well plates (3×10^4 cells) and transfected the next day with the various pGL4.24[*luc2*P/minP] vector constructs with or without the murine Etv2 expression plasmid (pMSCV-*Etv2*). Renilla luciferase vector (Promega) was cotransfected to normalize

transfection efficiency. Cells were harvested 48 h after transfection, and luciferase activity was measured using the Dual-Luciferase Reporter Assay kit and GloMax™ Systems (Promega). Reporter gene activities were first normalized to the Renilla luciferase value and further compared to that of the control pGL4.24 reporter. All luciferase in vitro experiments were repeated using at least four biological replicates.

To perform luciferase assays in zebrafish embryos, the embryos were injected at 1-cell stage with 25 pg of the pGL4.24 vector containing the putative enhancer. A subset of these embryos were also injected with 270 pg of zebrafish *etv2* mRNA (Sumanas and Lin, 2006) into the yolk. Embryos were incubated at 32°C and imaged at the 50% epiboly stage. 24 embryos from each injection group were loaded individually into the wells of a 96-well plate. 100 μl of CycLuc1 (Calbiochem), a synthetic luciferase substrate, was added to each well to the final concentration of 100 μM. 10 minutes after the addition of substrate, the embryos were imaged with a 5-min exposure in an IVIS Lumines LT Series III In Vivo Imaging System. Luminescence for each embryo was quantified in ImageJ. Relative fluorescence intensity was calculated by subtracting background and dividing the average fluorescence intensity in embryos co-injected with *etv2* mRNA and a luciferase construct over the fluorescence intensity in control embryos injected with a luciferase construct only.

To test the requirement of the ETS sites in two selected *flt4* enhancers, a mutagenized enhancer DNA with all ETS sites mutated was synthesized by gene synthesis (Genscript) and subcloned into the pGL4.24 vector (sequences listed in Table S1). For luciferase assays, the same dose of mutated and wild-type *flt4* constructs was co-injected with *etv2* mRNA in the same experiment. Each experiment was repeated at least twice.

RESULTS

Etv2 expression is increased in a subset of venous endothelial cells during initiation of lymphangiogenesis

To test for a potential role of *etv2* in lymphangiogenesis, we first used *in situ* hybridization and confocal imaging of Tg(-2.3 *etv2:GFP*)^{zf372} reporter line expression (Veldman and Lin, 2012) to analyze *etv2* expression in wild-type zebrafish embryos and larvae at 24-56 hpf when lymphangiogenesis is initiated. Significant *etv2* expression in the dorsal aorta (DA), posterior cardinal vein (PCV), and intersegmental vessels (ISVs) was observed at 24 hpf (Fig. 1A,D,G). Interestingly, *etv2* expression appeared less intense in the DA (arrows) compared to the PCV at 48-56 hpf (Fig. 1B,C,E,F,H,I). In addition, *etv2* expression was present in ISVs including venous-derived ISVs at 48 and 56 hpf (Fig. 1H,I).

We then analyzed whether *etv2* expression overlapped with *prox1a* expression using the vascular endothelial reporter TgBAC(*etv2:GFP*)^{ci1} (Proulx et al., 2010) and the lymphatic reporter TgBAC(*prox1a:KalT4-UAS:uncTagRFP*)^{nim5} (Dunworth et al., 2014), hereafter referred to as *prox1a:RFP.* Indeed, we observed co-localization of GFP and RFP in putative lymphatic endothelial progenitor cells at 24 hpf (Fig. S1A–D) and the thoracic duct and intersegmental lymphatic vessels (ISLVs) at 4.5 dpf (Fig. S1E–H). The expression of *etv2* in lymphatic progenitor cells suggested its potential role in lymphangiogenesis.

Etv2 depletion inhibits thoracic duct formation

We first analyzed lymphangiogenesis in *etv2*^{y11} null mutants, which undergo significant recovery of vascular development at later stages, although they exhibit nearly complete inhibition of early vasculogenesis (Craig et al., 2015; Pham et al., 2007). The major lymphatic vessel, the thoracic duct (TD), was completely absent in *etv2* mutant larvae, as evident from the lymphatic reporter *prox1a:RFP* expression (Fig. 2).

Because *etv2*^{y11} mutants show defects in early vasculogenesis, which may indirectly affect lymphangiogenesis, we used a previously validated photoactivatable *etv2* morpholino (MO) to inhibit Etv2 function during later stages of embryogenesis, after the formation of major axial vessels. In this design, a photosensitive caging strand was hybridized to a translation-blocking *etv2* antisense MO, rendering it inactive (Tomasini et al., 2009). We have previously demonstrated that photoactivation of *etv2* MO by exposure to UV light at progressive stages of development resulted in vascular phenotypes with different levels of severity as well as inhibition of *etv2*:GFP expression (Kohli et al., 2013). However, as we previously demonstrated, photoactivation of *etv2* MO at the 18-somite (18 hpf) and later stages resulted in no apparent defects in blood vessel development due to its functional redundancy with Fli1b (Craig et al., 2015). To analyze the role of Etv2 during lymphatic development, we performed functional Etv2 knockdown by photoactivatable MO injection into embryos from the *fli1a:GFP; kdrl:mCherry* line and analyzed the formation of the thoracic duct (Fig. 3A–D′). Control uninjected embryos demonstrated normal blood vessel and lymphatic development (Fig. 3A,A′) as did those embryos injected with caged *etv2* MO, but never exposed to UV photoactivation (Fig. 3B,B′). As expected, embryos photoactivated at the shield stage (6 hpf), prior to the onset of vasculogenesis, demonstrated defective vascular endothelial development (Fig. 3C,C′, compare with Fig. 2), effectively recapitulating the vascular phenotype observed in *etv2*^{y11} genetic mutants (Craig et al., 2015; Pham et al., 2007), which further supports the specificity of the observed MO phenotype. Inhibition of Etv2 function at 24 hpf, after the major axial vessels have already formed, specifically affected lymphangiogenesis without affecting vascular development. The major lymphatic vessel, the thoracic duct (TD), was absent or discontinuous in Etv2-depleted larvae, while the major axial and secondary intersegmental blood vessels (ISVs) were not affected (Fig. 3D,D′). Similar absence of the thoracic duct was observed in Etv2-depleted larvae at 5 and 7 dpf using *prox1a:RFP* reporter line (Fig. 3E–H, Fig. S2A–D). This data also argues that the failure of thoracic duct formation at 5 dpf is not due to developmental delay. No other defects in embryonic development were observed in Etv2-depleted larvae. Injection and photoactivation of a control MO did not cause any defects in lymphatic development (Fig. S2E,F). Photoactivation of caged Etv2 MO at 34 or 48 hpf also did not affect the thoracic duct formation or *prox1a:RFP* expression (Fig. S2G,H), suggesting that Etv2 function is required at the initial stage of lymphangiogenesis.

As an additional test for the specificity of caged *etv2* MO phenotype, we examined lymphatic defects in wild-type and *etv2* heterozygous mutant embryos and larvae, obtained from the incross of *etv2*^{y11} heterozygous carriers, and injected with a reduced dose of caged *etv2* MO, which was photoactivated at 24 hpf. The larvae were blindly scored for the defects in the thoracic duct at 5 dpf and subsequently genotyped. The thoracic duct was largely

normal in 84% of wild-type larvae, while 46 % of the *etv2*$^{+/-}$ larvae displayed discontinuous or absent thoracic ducts ($p<0.01$) (Fig. S3). These results demonstrate that *etv2* heterozygous embryos have increased sensitivity to the low dose of *etv2* MO, and further support the specificity of the caged *etv2* MO lymphatic phenotype.

Etv2 depletion inhibits formation of lymphatic progenitors

We then analyzed if the lymphatic progenitors, parachordal lymphangioblasts (PLs), failed to migrate from the PCV in the absence of Etv2 function. Control uninjected *fli1a:GFP; kdrl:mCherry* reporter zebrafish and control morpholino-injected but not photoactivated larvae showed normal migration of PLs when analyzed by confocal microscopy at 56 hpf (Fig. 3I,J,I′,J′). As expected, embryos injected with caged Etv2 MO and exposed to UV photoactivation at the shield stage (6 hpf), prior to initiation of vasculogenesis, developed abnormal vasculature, while PLs could not be clearly visualized due to abnormal branching of ISVs (Fig. 3K,K′). However, embryos where Etv2 depletion occurred at 24 hpf developed normal vasculature compared to control embryos but no PLs (Fig. 3L,L′, arrowheads). Interestingly, the formation of venous ISVs was not affected in the majority of Etv2 depleted larvae, while the sprouting of lymphatic-fated cells from the PCV was inhibited (Fig. 4, Fig. S4A, Movies 1 and 2). Larvae where Etv2 has been knocked down demonstrate normal venous sprouting, along with stalled or collapsing PL sprouts that have not migrated by 75 hpf (Movie 2, blue arrowheads) compared to wild type larvae (Movie 1) where migration is complete by 56 hpf. In some cases where PL sprouts have reached the horizontal myoseptum, PLs appear to stall and fail to migrate along the myoseptum (Movie 2). Additionally, we analyzed the numbers of early *prox1a*$^{+}$ lymphatic progenitors in the PCV in the TgBAC(*prox1a:KalT4-UAS:uncTagRFP*) reporter line, crossed with the Tg(UAS:GFP) reporter line (Asakawa et al., 2008), as GFP expression is visible much earlier than RFP expression (this double transgenic line is further labeled as *prox1a:GFP*). We observed a significant decrease in the number of *prox1a:GFP*$^{+}$ cells in the PCV of *etv2* depleted embryos compared to uninjected embryos (Fig. 5, Fig. S4B).

Etv2 inducible knockdown results in decreased expression of genes associated with lymphangiogenesis

In order to further examine the role of Etv2 during embryonic lymphangiogenesis, the expression of *flt4* and lymphatic vessel endothelial hyaluronan receptor 1 (*lyve1b*) (Okuda et al., 2012) was examined in Etv2 depleted larvae by *in situ* hybridization at 56 hpf. Expression of both markers is restricted to the PCV and is thought to label both venous endothelial cells and lymphatic progenitors at this stage (Fig. 6A,E) (Okuda et al., 2012). Similar to controls, expression of *flt4* and *lyve1b* was not affected in the embryos that were injected with caged morpholino solution, but never exposed to UV light (Fig. 6B,F). As expected, early Etv2 knockdown at the shield stage (6 hpf) resulted in the loss of *flt4* and *lyve1b* expression (Fig. 6C,G). However, those embryos depleted of Etv2 at 24 hpf showed greatly decreased expression of *flt4* and *lyve1b* (Fig. 6D,H). In contrast, late Etv2 depletion by photoactivation (24 hpf) did not cause inhibition of vascular endothelial marker *fli1a* expression (Fig. 6I–L). As expected, *fli1a* expression in ISVs and ISV sprouting was inhibited after early photoactivation at 6 hpf (Fig. 6K). Taken together, these results argue that expression of markers associated with lymphangiogenesis is specifically lost when Etv2

function is inhibited at 24 hpf while expression of the generic vascular endothelial marker *fli1a* is not affected.

Heat shock inducible overexpression of Etv2 results in ectopic expression of genes associated with lymphangiogenesis

In light of the data implicating the role for Etv2 in lymphangiogenesis, we investigated whether the overexpression of *etv2* was sufficient to induce expression of markers associated with lymphangiogenesis. We previously demonstrated that *etv2* overexpression by mRNA or DNA injection induces precocious and ectopic expression of multiple vascular endothelial markers (Sumanas and Lin, 2006). Interestingly, greatly increased and precocious expression of *lyve1b* was also observed when *etv2* mRNA was injected (Wong et al., 2009). To avoid inducing early ubiquitous vascular endothelial marker expression, a heat-shock inducible Etv2 construct was used (Veldman et al., 2013). Embryos at 1-2 cell stage were injected with an *hsp70:Etv2-mCherry* overexpression construct and allowed to develop until 24 or 48 hpf when *etv2* overexpression was induced by heatshock. Embryos were then cultured to either 28-30 hpf (if heat-shocked at 24 hpf) or 54-56 hpf (if heat-shocked at 48 hpf) and fixed in order to examine marker expression by *in situ* hybridization. Embryos with heatshock-induced *etv2* overexpression showed ectopic expression of *flt4*, largely restricted to the somitic mesoderm compared to sibling uninjected controls (Fig. 7A,B, Fig. S5A,B) or uninjected heatshocked embryos, which did not demonstrate ectopic *flt4* expression (data not shown). In contrast, ectopic *lyve1b* expression in heat-shock *etv2* overexpressing embryos was largely limited to the cell layer overlying the yolk at both stages examined (Fig. 7C,D, Fig. S5C,D). The majority of *etv2*-overexpressing embryos did not show ectopic *fli1a* expression except for a small fraction (<10%) of embryos where a few scattered ectopic *fli1a*-positive cells were observed in the trunk region or over the yolk (Fig. 7E,F, Fig. S5E,F, and data not shown). No ectopic induction of *prox1a* expression was observed under these conditions (Fig. 7G,H, Suppl. Fig. S5G,H). It has been previously reported that heat-shock inducible *etv2* overexpression can induce vascular marker expression in the somitic tissue (Veldman et al., 2013), similar to the observed *flt4* expression. Additional tissue-specific factors may account for the observed differences between *flt4* and *lyve1b* expression (see Discussion). Because *prox1a* expression was not induced using heat-shock specific promoter, we then tested if vascular endothelial overexpression of *etv2* was sufficient to increase expression of *prox1a*. However, injection of *fli1a:etv2-2A-mCherry* DNA construct (Casie Chetty et al., 2017) also did not result in an expansion of *prox1a*$^{+}$ cells in the vasculature (Fig. S6), suggesting that Etv2 may not be sufficient to directly induce *prox1a* expression.

Etv2 function is required for Vegfc-induced lymphangiogenesis

Vegfc overexpression is known to induce increased lymphangiogenesis (Le Guen et al., 2014). We then tested if the induction of ectopic lymphangiogenesis by Vegfc required Etv2 function. Formation of parachordal lymphangioblasts was analyzed in *fli1:GFP* reporter embryos co-injected with *hsp70:Vegfc* construct and caged *etv2* MO, followed by photoactivation at 24 hpf, and compared to embryos injected with either *hsp70:Vegfc* or caged *etv2* MO alone. The average number of PLs per segment was assessed by counting the number of PLs in ten intersegmental spaces (equivalent to the width of ten somites) over the

trunk of each larva. As expected, induction of Vegfc expression by heat-shock following the injection of an *hsp70:Vegfc* construct resulted in the precocious formation of parachordal lymphangioblasts (52 hpf vs. 56 hpf) and in larger numbers (4.67 PLs per segment, n=35 larvae analyzed) than in control uninjected larvae, which had very few PLs at 52 hpf (0.085 PLs per segment, n=49) (Fig. 8). Inhibition of *etv2* in Vegfc overexpressing embryos by caged MO photoactivation at 24 hpf resulted in a near complete absence of lymphangioblasts, with an average of 0.055 PL per segment (n=44 larvae) (Fig. 8E,G). These results argue that Vegfc fails to induce lymphangiogenesis in the absence of Etv2 function.

Etv2 directly binds to the promoter / enhancer regions of genes associated with lymphangiogenesis

To determine if Etv2 directly regulates the expression of genes associated with lymphangiogenesis, we analyzed results from a previously reported Etv2 ChIP-Seq, performed using *in vitro* differentiated mouse embryonic stem cells (ES) (Liu et al., 2015). This analysis revealed specific Etv2 binding peaks present within *Flt4, Prox1*, and *Lyve1* proximal promoter/enhancer regions (Fig. 9A, Table S1). We performed a luciferase reporter assay in 293T cells using the selected Etv2 putative binding sites and found that the Etv2 putative enhancers from *Flt4, Prox1*, and *Lyve1* genes activated the luciferase reporter expression in the presence of mouse Etv2 (Fig. 9B, Fig. S7). To test the activity of these putative enhancers *in vivo*, we injected wild type zebrafish embryos at the 1-cell stage with luciferase reporters containing mouse enhancers with putative Etv2 binding sites with or without zebrafish *etv2* mRNA, and performed luciferase assay at 6 hpf, prior to the initiation of the endogenous *etv2* expression. All three *Flt4* enhancers and the *Lyve1* enhancer greatly activated luciferase reporter expression in the presence of zebrafish Etv2 (Fig. 9C, Fig. S8). Interestingly, *Prox1* enhancer failed to activate luciferase reporter expression in zebrafish embryos and its activity was also relatively low (~2.5 fold induction in the presence of Etv2 compared to -Etv2) in 293T cells. To test if ETS sites were required for the reporter activation by Etv2, the constructs with the mutated consensus ETS binding sites were made for two selected *Flt4* enhancers. Mutating the putative ETS binding sites in the *Flt4* enhancers greatly reduced luciferase reporter expression in the zebrafish assay (Fig. 9C, Fig. S8). These data suggest that Etv2 activates *flt4* and *lyve1b* expression by directly binding to its promoter / enhancer regions, and that the function of these enhancers is conserved among different vertebrates.

Vascular endothelial cell specific overexpression of *flt4* is not sufficient to rescue lymphangiogenesis defects in Etv2 depleted embryos

Our results suggest that Etv2 may promote lymphangiogenesis by upregulating or maintaining *flt4* expression. Therefore, we tested if *flt4* expression was sufficient to rescue the lymphangiogenesis defects in Etv2-deficient embryos by injecting a construct expressing *flt4-2a-mCherry* in vascular endothelial cells under the *fli1a* promoter. As we previously observed, knockdown of *etv2* at 24 hpf results in a reduction in the number of *prox1a:GFP*$^{+}$ cells in the PCV at 30 hpf compared to uninjected embryos (Fig. S9A,B). Injection of the *flt4* overexpression construct did not rescue this population of *prox1a:GFP*$^{+}$ cells in *etv2* knockdown embryos (Fig. S9D–D′) and interestingly resulted in reduced numbers of *prox1a*

$^{+}$ cells in embryos that were not injected with the Photomorph solution (Fig. S9C–C′). We obtained a stable *fli1a:flt4-2a-mCherry* transgenic line and analyzed thoracic duct formation. Thoracic ducts were absent or discontinuous in *fli1a:flt4-mCherry* larvae at 5 dpf (Fig. S9F–G′), suggesting that venous specific *flt4* expression is important for lymphangiogenesis, and that its misexpression throughout the vasculature inhibits lymphatic development.

DISCUSSION

Our results demonstrate that Etv2 is required for lymphangiogenesis in zebrafish independently from its previously reported role in vasculogenesis. Through a series of experiments designed to test the temporal relationship of *etv2* to lymphatic vessel development, while controlling for potential off-target effects, we show that Etv2 depletion after vasculogenesis inhibits normal development of the major lymphatic vessel, the thoracic duct, as well as lymphatic precursor cells, without affecting vascular development. Our results further demonstrate that Etv2 directly upregulates expression of *flt4*, the function of which is required for lymphangiogenesis, and thus functions as one of the key regulators of initiating lymphangiogenesis.

It has previously been reported that *etv2* is downregulated after 24 hpf by a putative microRNA-mediated post transcriptional process (Moore et al., 2013). Based on inducible knockdown of *etv2* using UV-activated caged MO, it was argued that while *etv2* is essential for endothelial cell commitment, it becomes dispensable for later steps of vascular development. However, the previous study also reported no vascular expression of Etv2 protein at 24 hpf or 48 hpf, in contrast to our findings of *etv2* vascular expression in transgenic fluorescent reporter and mRNA expression in wild-type embryos or larvae at 24-56 hpf by *in situ* hybridization. There are possible explanations for these differences. First, immunohistochemistry sensitivity could be limited, such that low-level protein may not be detected under those study conditions. The earlier study utilized conditional knockdown of *etv2* at stages prior to and during vasculogenesis, and measured outcomes of blood vascular development up to 24 hpf. In contrast, in our study, the conditional knockdown of *etv2* occurred at a stage after major axial blood vessel development and measured outcomes were related to lymphatic vessel development. The previous study utilized a different method of UV-activated caged MO, and it is possible that our caged MO (Photomorph solution) demonstrated higher efficiency. Our study continues to evaluate *etv2* effects up to 7 dpf, whereas the previous study had endpoints at 48 hpf, which demonstrated a relative decline in Etv2 presence but not its eradication; therefore, our findings largely correlate with the overall results of the previous study. We demonstrate in this study that *etv2* becomes an active participant in the determination of lymphatic endothelial cell fate. Interestingly, *etv2* is present in both the dorsal aorta and the posterior cardinal vein, as well as developing ISVs at 24 hpf. The staining over the aorta is decreased in later stages, while becoming enriched in the ventral wall of the PCV at 48 hpf. The regularly spaced and discontinuous pattern of venous enrichment is intriguing, and provokes speculation that Etv2 expression might correlate with cells involved in lymphangiogenesis. Indeed, *prox1a*-positive lymphangioblasts have been shown to originate within the ventral wall of the PCV at similar embryonic stages (Nicenboim et al., 2015).

Taken as a whole, the above results demonstrate the requirement of *etv2* for lymphangiogenesis. Previous *in vitro* data have demonstrated that mouse *Flt4* enhancer contains an evolutionarily conserved FOX:ETS domain that is bound by Etv2 and FoxC2 transcription factors (De Val et al., 2008); therefore, *Flt4* is a likely direct target of Etv2. Our results show that zebrafish *flt4* expression is greatly reduced in Etv2 inhibited larvae. Furthermore, *vegfc* overexpression fails to increase the number of lymphangioblasts in Etv2 inhibited larvae. ChIP-Seq analysis shows direct binding of Etv2 to *Flt4* enhancers. These results are supported by the *in vivo* luciferase assay, which shows activation of murine *Flt4* enhancers by zebrafish *etv2* mRNA in zebrafish embryos. This also demonstrates that the activity of these enhancers is conserved evolutionarily in different species.

Our data further demonstrate that Etv2 is sufficient to induce ectopic expression of *flt4* and *lyve1b.* Ectopic *flt4* expression was mostly restricted to the somites. This phenotype is quite similar to the previously observed induction of vascular markers upon *hsp70:Etv2* overexpression (Veldman et al., 2013). Unexpectedly, ectopic *lyve1b* expression was restricted to the cells that overlay the yolk, and was not apparent in the somites. It is possible that additional factors may be required for *lyve1b* induction which are not expressed in the somites, or certain repressors may be present in the somitic tissue which repress *lyve1b* but are permissive for *flt4* expression. The nature of ectopic *lyve1b*-expressing cells is currently unclear and will require further investigation.

These results support the model where Etv2 directly regulates *flt4* expression within the PCV prior to the initiation of lymphangiogenesis. However, endothelial *flt4* expression failed to rescue lymphangiogenesis in Etv2 inhibited embryos and larvae. It is possible that the endogenous *flt4* expression level is not well recapitulated using the *fli1a* promoter, which would also express *flt4* in the artery in addition to its normal venous expression. Indeed, *fli1a:flt4* transgenic embryos and larvae show reduction of *prox1a*-positive cells and absence of the thoracic duct, arguing that venous-specific *flt4* expression is important for lymphangiogenesis. It is also possible that *flt4* is expressed at a higher level in our transgenic model and may sequester Vegfc during early developmental stages, resulting in insufficient Vegfc levels during the critical stages of lymphangiogenesis. However, it is also likely that Etv2 directly activates the expression of multiple genes associated with lymphangiogenesis. Indeed, ChIP-seq results show that Etv2 can directly bind to the *Lyve1* enhancer. Similarly, Etv2 activated *Lyve1* enhancer in a luciferase reporter assay, arguing that Etv2 directly regulates *Lyve1* expression. It is likely that Etv2 may also activate additional yet to be identified targets involved in lymphangiogenesis.

An important question is whether Etv2 directly activates *prox1a* expression. The number of *prox1a* progenitors was reduced but not completely absent in Etv2 depleted embryos. However, no ectopic induction of *prox1a* expression was observed upon *hsp:Etv2* expression or in the *fli1a:etv2* transgenic line (data not shown). ChIP-Seq results show Etv2 binding to the *Prox1* enhancer. However, this *Prox1* enhancer was activated relatively weakly (2.5-fold) *in vitro*, and was not activated in zebrafish embryos. Therefore, while we cannot exclude the possibility that Etv2 may regulate *prox1a* expression through different enhancers, our data do not support direct regulation of *prox1a* expression by Etv2 in zebrafish embryos at present. The loss of *prox1a*-positive lymphatic progenitors in Etv2 depleted embryos can be

explained by the inhibition of Flt4 expression. Vegfc-Flt4 signaling is known to promote proliferation of lymphatic progenitors and a similar loss of *prox1a* progenitors was observed in Vegfc and Flt4-inhibited embryos (Koltowska et al., 2015).

In addition to the absence of parachordal lymphangioblasts and the thoracic duct, *vegfc* and *flt4* zebrafish mutants have reduced or absent venous sprouting (Hogan et al., 2009b; Villefranc et al., 2013), while we did not detect apparent defects in venous sprouting in Etv2 knockdown larvae, despite the significant loss of *flt4* expression. Importantly, in our experiments, Etv2 function is only inhibited at 24 hpf, and *flt4* expression would only be reduced at even later stages, while in *flt4* mutants its function is absent throughout the embryogenesis. It is possible that Flt4 has differential timing requirements in the venous and lymphatic sprouting which has not been previously investigated. Alternatively, a reduced level of *flt4* present in Etv2 knockdown embryos could be sufficient for venous sprouting but insufficient for lymphangioblast migration. In support of this model, *vegfc* mutant larvae have been reported to display a complete absence of the thoracic duct but only a partial reduction in venous sprouting (Villefranc et al., 2013), suggesting that lymphatic and venous sprouting have differential requirements for Vegfc signaling.

In summary, our results identify Etv2 as a novel and previously unexplored regulator of lymphatic vessel development. Since Etv2 function is highly evolutionarily conserved, it is tempting to speculate that Etv2 may have a similar function during mammalian lymphangiogenesis, which is supported by ChIP-Seq data analysis of the mouse Etv2 protein binding to the promoter / enhancer regions of multiple genes involved in lymphangiogenesis. However, further research will be necessary to establish if Etv2 role is conserved during mammalian lymphangiogenesis and if it is possible to target Etv2 as a novel therapeutic approach for treating different lymphatic disorders.

Supplementary Material

Refer to Web version on PubMed Central for supplementary material.

Acknowledgments

We thank Matthew Kofron and Michael Muntifering of the Cincinnati Children's Imaging Core (CCIC) for their expertise in confocal imaging, Ben Hogan for providing *hsp70:vegfc* constructs, and Monica Beltrame for providing *in situ* constructs, and Suk-Won Jin and Elke Ober for the *prox1a* reporter line.

Funding

This work was supported by the St. Baldrick's Foundation (award to J.A.D.), Cincinnati Children's Hospital Medical Center Procter Scholar Award (J.A.D.), National Institutes of Health [R01 HL107369 and R21 AI128445 to S.S., R01 HL55337 and R01 HL63736 to K.C., F31 HL135986 to A.L.K. and appointment of A.L.K. to T32 HL125204] and pilot awards from Cancer Free Kids and Ohio Cancer Research Associates (to S.S.).

References

Asakawa K, Suster ML, Mizusawa K, Nagayoshi S, Kotani T, Urasaki A, Kishimoto Y, Hibi M, Kawakami K. Genetic dissection of neural circuits by Tol2 transposon-mediated Gal4 gene and enhancer trapping in zebrafish. Proc Natl Acad Sci U S A. 2008; 105:1255–1260. [PubMed: 18202183]

Casie Chetty S, Rost MS, Enriquez JR, Schumacher JA, Baltrunaite K, Rossi A, Stainier DY, Sumanas S. Vegf signaling promotes vascular endothelial differentiation by modulating etv2 expression. Dev Biol. 2017; 424:147–161. [PubMed: 28279709]

Cermenati S, Moleri S, Neyt C, Bresciani E, Carra S, Grassini DR, Omini A, Goi M, Cotelli F, Francois M, Hogan BM, Beltrame M. Sox18 genetically interacts with VegfC to regulate lymphangiogenesis in zebrafish. Arterioscler Thromb Vasc Biol. 2013; 33:1238–1247. [PubMed: 23520166]

Craig MP, Grajevskaja V, Liao HK, Balciuniene J, Ekker SC, Park JS, Essner JJ, Balciunas D, Sumanas S. Etv2 and Fli1b Function Together as Key Regulators of Vasculogenesis and Angiogenesis. Arterioscler Thromb Vasc Biol. 2015

De Val S, Chi NC, Meadows SM, Minovitsky S, Anderson JP, Harris IS, Ehlers ML, Agarwal P, Visel A, Xu SM, Pennacchio LA, Dubchak I, Krieg PA, Stainier DY, Black BL. Combinatorial regulation of endothelial gene expression by ets and forkhead transcription factors. Cell. 2008; 135:1053–1064. [PubMed: 19070576]

Dunworth WP, Cardona-Costa J, Bozkulak EC, Kim JD, Meadows S, Fischer JC, Wang Y, Cleaver O, Qyang Y, Ober EA, Jin SW. Bone morphogenetic protein 2 signaling negatively modulates lymphatic development in vertebrate embryos. Circ Res. 2014; 114:56–66. [PubMed: 24122719]

Ferdous A, Caprioli A, Iacovino M, Martin CM, Morris J, Richardson JA, Latif S, Hammer RE, Harvey RP, Olson EN, Kyba M, Garry DJ. Nkx2-5 transactivates the Ets-related protein 71 gene and specifies an endothelial/endocardial fate in the developing embryo. Proc Natl Acad Sci U S A. 2009; 106:814–819. [PubMed: 19129488]

Francois M, Caprini A, Hosking B, Orsenigo F, Wilhelm D, Browne C, Paavonen K, Karnezis T, Shayan R, Downes M, Davidson T, Tutt D, Cheah KS, Stacker SA, Muscat GE, Achen MG, Dejana E, Koopman P. Sox18 induces development of the lymphatic vasculature in mice. Nature. 2008; 456:643–647. [PubMed: 18931657]

Hogan BM, Bos FL, Bussmann J, Witte M, Chi NC, Duckers HJ, Schulte-Merker S. Ccbe1 is required for embryonic lymphangiogenesis and venous sprouting. Nat Genet. 2009a; 41:396–398. [PubMed: 19287381]

Hogan BM, Herpers R, Witte M, Helotera H, Alitalo K, Duckers HJ, Schulte-Merker S. Vegfc/Flt4 signalling is suppressed by Dll4 in developing zebrafish intersegmental arteries. Development. 2009b; 136:4001–4009. [PubMed: 19906867]

Isogai S, Hitomi J, Yaniv K, Weinstein BM. Zebrafish as a new animal model to study lymphangiogenesis. Anat Sci Int. 2009; 84:102–111. [PubMed: 19288175]

Jowett T. Analysis of protein and gene expression. Methods Cell Biol. 1999; 59:63–85. [PubMed: 9891356]

Karkkainen MJ, Haiko P, Sainio K, Partanen J, Taipale J, Petrova TV, Jeltsch M, Jackson DG, Talikka M, Rauvala H, Betsholtz C, Alitalo K. Vascular endothelial growth factor C is required for sprouting of the first lymphatic vessels from embryonic veins. Nat Immunol. 2004; 5:74–80. [PubMed: 14634646]

Kimmel CB, Ballard WW, Kimmel SR, Ullmann B, Schilling TF. Stages of embryonic development of the zebrafish. Dev Dyn. 1995; 203:253–310. [PubMed: 8589427]

Kohli V, Schumacher JA, Desai SP, Rehn K, Sumanas S. Arterial and venous progenitors of the major axial vessels originate at distinct locations. Dev Cell. 2013; 25:196–206. [PubMed: 23639444]

Koltowska K, Lagendijk AK, Pichol-Thievend C, Fischer JC, Francois M, Ober EA, Yap AS, Hogan BM. Vegfc Regulates Bipotential Precursor Division and Prox1 Expression to Promote Lymphatic Identity in Zebrafish. Cell Rep. 2015; 13:1828–1841. [PubMed: 26655899]

Kuchler AM, Gjini E, Peterson-Maduro J, Cancilla B, Wolburg H, Schulte-Merker S. Development of the zebrafish lymphatic system requires VEGFC signaling. Current biology : CB. 2006; 16:1244–1248. [PubMed: 16782017]

Lawson ND, Weinstein BM. In vivo imaging of embryonic vascular development using transgenic zebrafish. Dev Biol. 2002; 248:307–318. [PubMed: 12167406]

Le Guen L, Karpanen T, Schulte D, Harris NC, Koltowska K, Roukens G, Bower NI, van Impel A, Stacker SA, Achen MG, Schulte-Merker S, Hogan BM. Ccbe1 regulates Vegfc-mediated induction

of Vegfr3 signaling during embryonic lymphangiogenesis. Development. 2014; 141:1239–1249. [PubMed: 24523457]

Lee D, Park C, Lee H, Lugus JJ, Kim SH, Arentson E, Chung YS, Gomez G, Kyba M, Lin S, Janknecht R, Lim DS, Choi K. ER71 acts downstream of BMP, Notch, and Wnt signaling in blood and vessel progenitor specification. Cell Stem Cell. 2008; 2:497–507. [PubMed: 18462699]

Liu F, Li D, Yu YY, Kang I, Cha MJ, Kim JY, Park C, Watson DK, Wang T, Choi K. Induction of hematopoietic and endothelial cell program orchestrated by ETS transcription factor ER71/ETV2. EMBO Rep. 2015; 16:654–669. [PubMed: 25802403]

Moore JC, Sheppard-Tindell S, Shestopalov IA, Yamazoe S, Chen JK, Lawson ND. Post-transcriptional mechanisms contribute to Etv2 repression during vascular development. Dev Biol. 2013; 384:128–140. [PubMed: 24036310]

Nicenboim J, Malkinson G, Lupo T, Asaf L, Sela Y, Mayseless O, Gibbs-Bar L, Senderovich N, Hashimshony T, Shin M, Jerafi-Vider A, Avraham-Davidi I, Krupalnik V, Hofi R, Almog G, Astin JW, Golani O, Ben-Dor S, Crosier PS, Herzog W, Lawson ND, Hanna JH, Yanai I, Yaniv K. Lymphatic vessels arise from specialized angioblasts within a venous niche. Nature. 2015

Okuda KS, Astin JW, Misa JP, Flores MV, Crosier KE, Crosier PS. lyve1 expression reveals novel lymphatic vessels and new mechanisms for lymphatic vessel development in zebrafish. Development. 2012; 139:2381–2391. [PubMed: 22627281]

Pham VN, Lawson ND, Mugford JW, Dye L, Castranova D, Lo B, Weinstein BM. Combinatorial function of ETS transcription factors in the developing vasculature. Dev Biol. 2007; 303:772–783. [PubMed: 17125762]

Proulx K, Lu A, Sumanas S. Cranial vasculature in zebrafish forms by angioblast cluster-derived angiogenesis. Dev Biol. 2010; 348:34–46. [PubMed: 20832394]

Schulte-Merker S, Sabine A, Petrova TV. Lymphatic vascular morphogenesis in development, physiology, and disease. J Cell Biol. 2011; 193:607–618. [PubMed: 21576390]

Srinivasan RS, Geng X, Yang Y, Wang Y, Mukatira S, Studer M, Porto MP, Lagutin O, Oliver G. The nuclear hormone receptor Coup-TFII is required for the initiation and early maintenance of Prox1 expression in lymphatic endothelial cells. Genes Dev. 2010; 24:696–707. [PubMed: 20360386]

Sumanas S. Inducible Inhibition of Gene Function with Photomorpholinos. Methods Mol Biol. 2017; 1565:51–57. [PubMed: 28364233]

Sumanas S, Jorniak T, Lin S. Identification of novel vascular endothelial-specific genes by the microarray analysis of the zebrafish cloche mutants. Blood. 2005; 106:534–541. [PubMed: 15802528]

Sumanas S, Lin S. Ets1-related protein is a key regulator of vasculogenesis in zebrafish. PLoS Biol. 2006; 4:e10. [PubMed: 16336046]

Tammela T, Alitalo K. Lymphangiogenesis: Molecular mechanisms and future promise. Cell. 2010; 140:460–476. [PubMed: 20178740]

Tao S, Witte M, Bryson-Richardson RJ, Currie PD, Hogan BM, Schulte-Merker S. Zebrafish prox1b mutants develop a lymphatic vasculature, and prox1b does not specifically mark lymphatic endothelial cells. PLoS One. 2011; 6:e28934. [PubMed: 22216143]

Thompson MA, Ransom DG, Pratt SJ, MacLennan H, Kieran MW, Detrich HW 3rd, Vail B, Huber TL, Paw B, Brownlie AJ, Oates AC, Fritz A, Gates MA, Amores A, Bahary N, Talbot WS, Her H, Beier DR, Postlethwait JH, Zon LI. The cloche and spadetail genes differentially affect hematopoiesis and vasculogenesis. Dev Biol. 1998; 197:248–269. [PubMed: 9630750]

Tomasini AJ, Schuler AD, Zebala JA, Mayer AN. PhotoMorphs: a novel light-activated reagent for controlling gene expression in zebrafish. Genesis. 2009; 47:736–743. [PubMed: 19644983]

van Impel A, Zhao Z, Hermkens DM, Roukens MG, Fischer JC, Peterson-Maduro J, Duckers H, Ober EA, Ingham PW, Schulte-Merker S. Divergence of zebrafish and mouse lymphatic cell fate specification pathways. Development. 2014; 141:1228–1238. [PubMed: 24523456]

Veldman MB, Lin S. Etsrp/Etv2 is directly regulated by Foxc1a/b in the zebrafish angioblast. Circ Res. 2012; 110:220–229. [PubMed: 22135404]

Veldman MB, Zhao C, Gomez GA, Lindgren AG, Huang H, Yang H, Yao S, Martin BL, Kimelman D, Lin S. Transdifferentiation of fast skeletal muscle into functional endothelium in vivo by transcription factor Etv2. PLoS Biol. 2013; 11:e1001590. [PubMed: 23853546]

Villefranc JA, Nicoli S, Bentley K, Jeltsch M, Zarkada G, Moore JC, Gerhardt H, Alitalo K, Lawson ND. A truncation allele in vascular endothelial growth factor c reveals distinct modes of signaling during lymphatic and vascular development. Development. 2013; 140:1497–1506. [PubMed: 23462469]

Wigle JT, Oliver G. Prox1 function is required for the development of the murine lymphatic system. Cell. 1999; 98:769–778. [PubMed: 10499794]

Wong KS, Proulx K, Rost MS, Sumanas S. Identification of vasculature-specific genes by microarray analysis of etsrp/etv2 overexpressing zebrafish embryos. Dev Dyn. 2009; 238:1836–1850. [PubMed: 19504456]

Yang Y, Garcia-Verdugo JM, Soriano-Navarro M, Srinivasan RS, Scallan JP, Singh MK, Epstein JA, Oliver G. Lymphatic endothelial progenitors bud from the cardinal vein and intersomitic vessels in mammalian embryos. Blood. 2012; 120:2340–2348. [PubMed: 22859612]

Yaniv K, Isogai S, Castranova D, Dye L, Hitomi J, Weinstein BM. Live imaging of lymphatic development in the zebrafish. Nat Med. 2006; 12:711–716. [PubMed: 16732279]

Yoshimatsu Y, Yamazaki T, Mihira H, Itoh T, Suehiro J, Yuki K, Harada K, Morikawa M, Iwata C, Minami T, Morishita Y, Kodama T, Miyazono K, Watabe T. Ets family members induce lymphangiogenesis through physical and functional interaction with Prox1. J Cell Sci. 2011; 124:2753–2762. [PubMed: 21807940]

Highlights

- Etv2 expression is enriched in the vein during zebrafish lymphangiogenesis
- Inducible Etv2 knockdown inhibits lymphangiogenesis
- Blood vessels are not affected by Etv2 knockdown at 24 hpf
- Vegfc fails to induce lymphangiogenesis in Etv2 knockdown embryos
- Etv2 directly binds to Flt4 promoter and promotes its expression

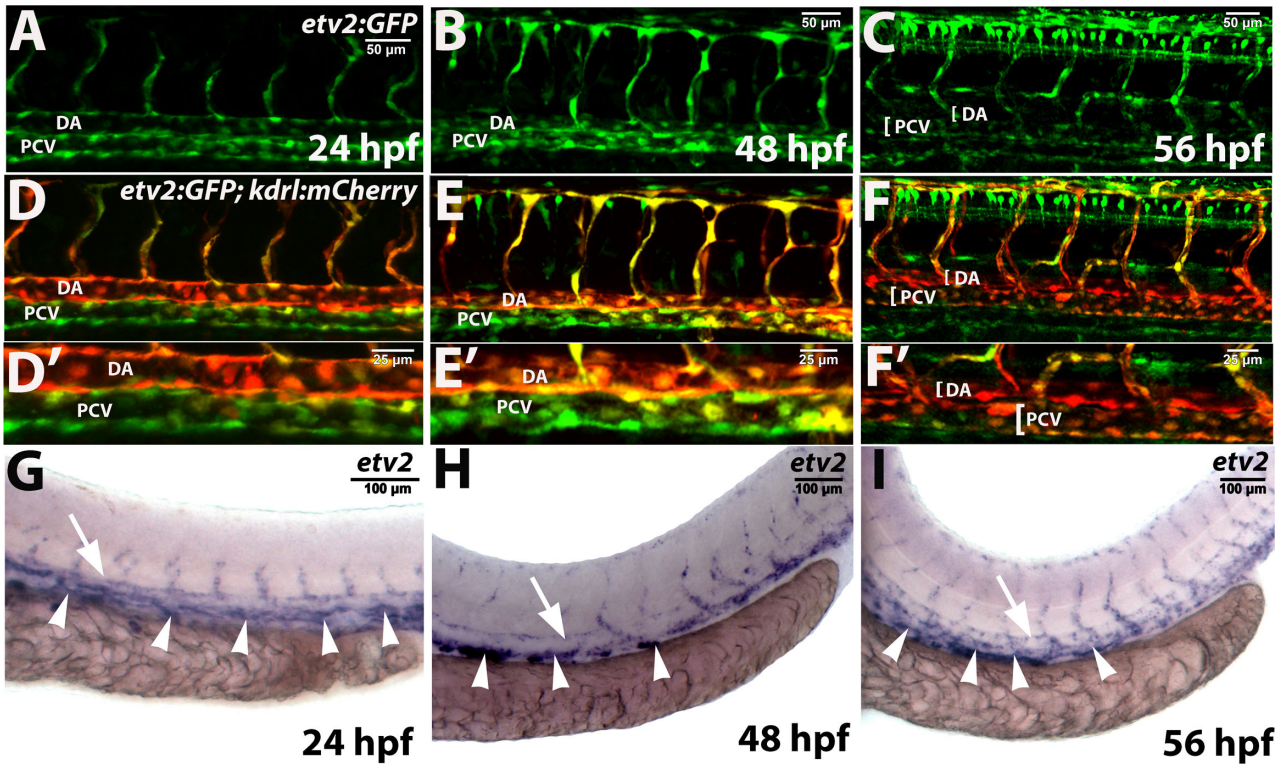

Figure 1. *Etv2* expression in wild type embryos and larvae as analyzed by the transgenic reporter expression and *in situ* hybridization

(A–F) Confocal images of Tg(-2.3kb *etv2:GFP; kdrl:mCherry)* reporter line at 24-56 hpf. Note that *etv2:GFP* expression is downregulated in the dorsal aorta (DA) at 48-56 hpf but is present in multiple cells in the posterior cardinal vein (PCV). (A–C) and (D–F) show the same embryos and larvae in green and overlaid green and red channels. (D′–F′) are higher magnification images of the DA and PCV from embryos and larvae in (D–F). Non-specific expression of *etv2:GFP* in neural cells is also apparent in (C,F). (G–I) In situ hybridization analysis of *etv2* expression at 24-56 hpf. Note the enriched *etv2* expression in the PCV (arrowheads) as compared to the DA (arrows) at 48-56 hpf. Each assay has been repeated at least twice with over 10 embryos or larvae analyzed in each group.

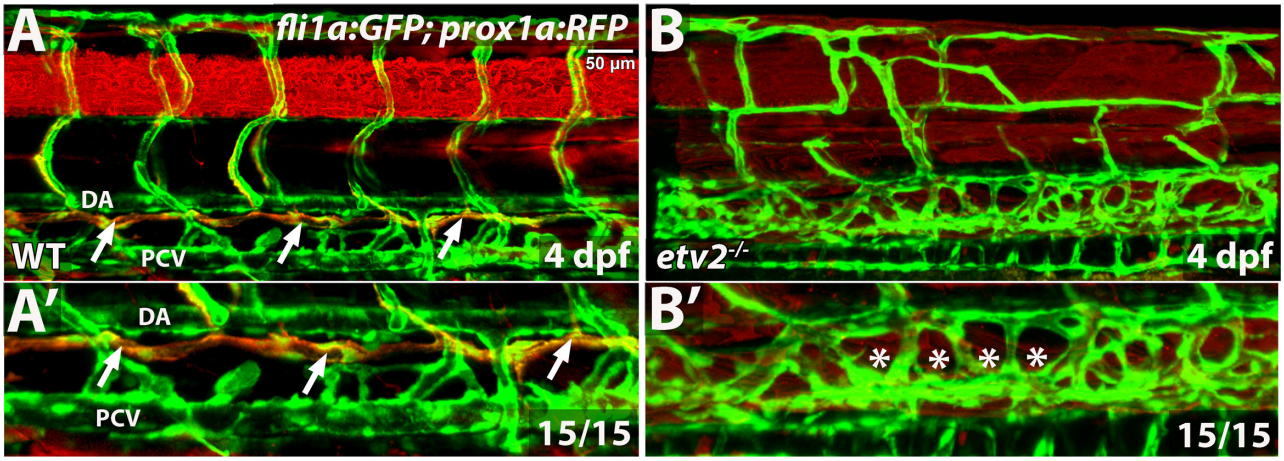

Figure 2. Thoracic duct is absent in *etv2* mutant larvae

Confocal microscopy analysis of the thoracic duct (arrows) in wild-type siblings and *etv2* mutant larvae in *fli1a:GFP; prox1a:RFP* background at 4 dpf. Note the absence of the thoracic duct (asterisks) and abnormal vascular patterning in *etv2* mutants. (A′,B′) Higher magnification images of larvae in A,B. DA, dorsal aorta, PCV, posterior cardinal vein.

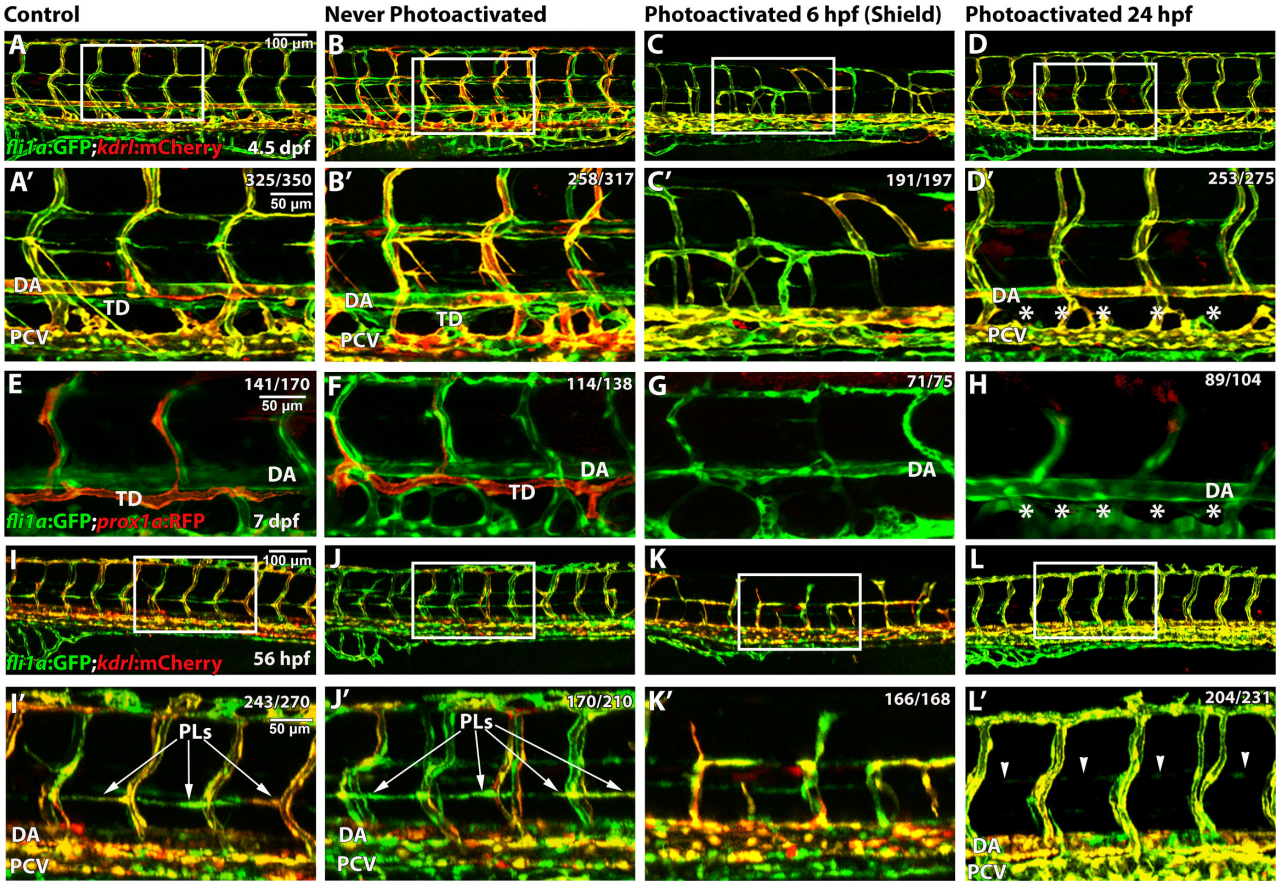

Figure 3. Etv2 depletion by caged MO photoactivation inhibits lymphangiogenesis

(A–H) Etv2 depletion by caged MO photoactivation inhibits thoracic duct development in *fli1a:GFP; kdrl:mCherry* (A–D′) and TgBAC*(prox1a:KalT4-UAS:uncTagRFP)* (E–H) reporter zebrafish larvae at 4.5 dpf and 7 dpf, respectively. (A,E) Control uninjected larvae with normal thoracic duct (TD) below the dorsal aorta (DA). (B,F) Embryos injected with *etv2* MO and caging strand solution (hereafter called “photomorph solution”), but never exposed to UV photoactivation, develop normal thoracic duct similar to uninjected controls. (C,G) Embryos injected with photomorph solution and exposed to UV photoactivation at 6 hpf (shield stage), develop abnormal vasculature (C) and no or discontinuous thoracic duct (G) compared to control embryos as expected. (D,H) Embryos injected with photomorph solution, exposed to UV photoactivation at 24 hpf, develop normal vasculature compared to control embryos but discontinuous or absent TD (asterisks). (I–L′) Etv2 is required for the formation of parachordal lymphangioblasts, as observed in *fli1a:GFP; kdrl:mCherry* reporter zebrafish larvae at 56 hpf. (I) Control uninjected larvae. (J) Embryos injected with photomorph solution, but never exposed to UV photoactivation, develop normal parachordal lymphangioblasts (PL, arrowheads) similar to uninjected controls. (K) Embryos injected with photomorph solution, and UV photoactivated at 6 hpf (shield stage), develop abnormal vasculature, while PLs cannot be visualized due to abnormal branching of ISVs. (L) Embryos injected with photomorph solution, and UV photoactivated at 24 hpf, develop normal vasculature compared to control embryos while PLs are absent (arrowheads). A′–D′ and I′–L′ show magnified areas indicated by boxes in A–D and I–L. Each experiment has

been repeated at least three times. Number of larvae showing a displayed phenotype out of the total number of larvae is shown in the upper right corner.

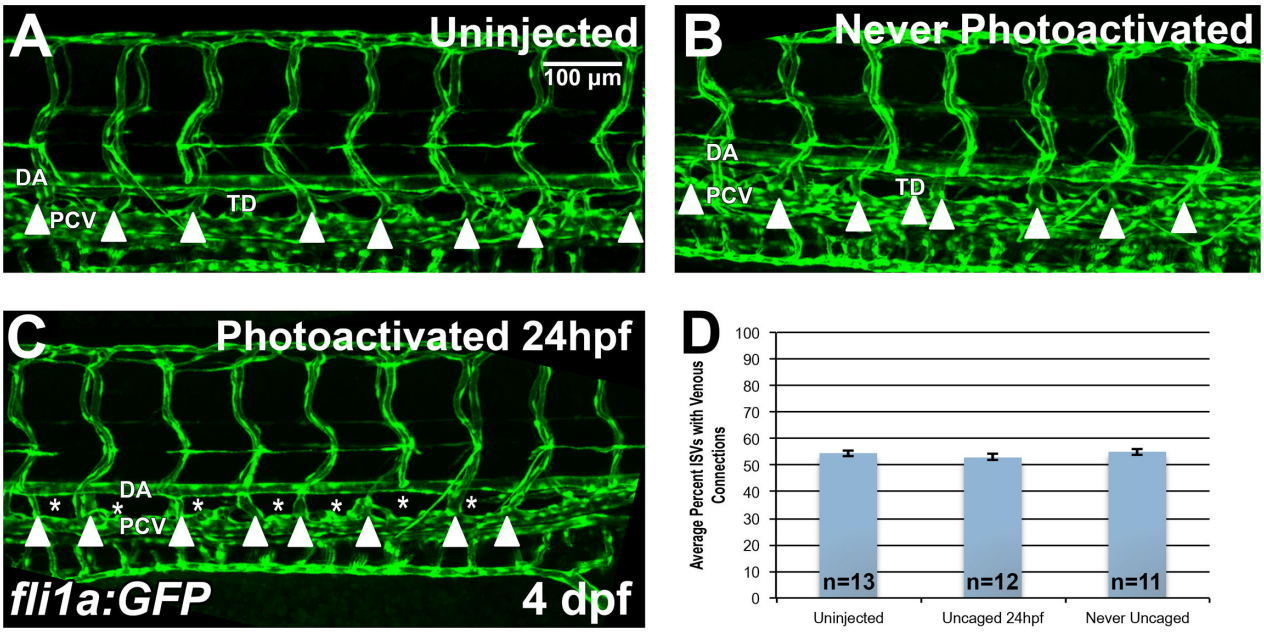

Figure 4. Etv2 depletion by caged MO photoactivation inhibits lymphangiogenesis but not the formation of venous intersegmental vessels (ISVs)

(A–D) Analysis of venous ISVs in *fli1a:GFP* larvae at 4 dpf. (A) Control uninjected larva at 4 dpf, with the thoracic duct (TD) located below the dorsal aorta (DA). Embryos injected with photomorph solution and never photoactivated develop normal TD and vasculature (B), while injected embryos UV photoactivated at 24 hpf (C), develop normal vasculature compared to control embryos, while the thoracic duct is absent (asterisks) at 4 dpf. Note that the venous derived intersegmental vessels are present in both control and Etv2-inhibited larvae (arrowheads). (D) Quantification of percent of ISVs with venous connection at 4 dpf in control uninjected larvae (54.5±1.2%, n=13) compared to never photoactivated (55.1±1.2%, n=11, p=0.74, two tailed Student's t-test) and 24 hpf photoactivated (52.9±1.2%, n=12, p=0.34, two tailed Student's t-test) larvae, indicates no significant difference between groups. Mean±SEM is shown. Individual data points are shown in Fig. S4A. This experiment has been replicated 3 times.

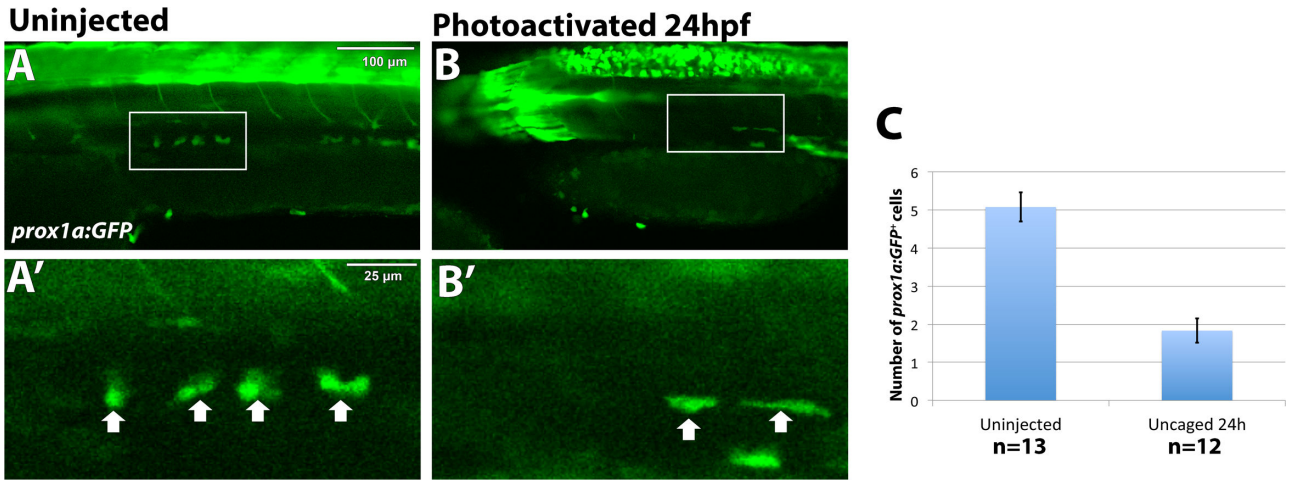

Figure 5. Etv2 depletion by caged MO photoactivation results in reduction of *prox1a:GFP*$^{+}$ lymphatic progenitor cells

TgBAC(*prox1a:KalT4-UAS:uncTagRFP); Tg(UAS:GFP)* live embryos were imaged by confocal microscopy at 32 hpf. The number of *prox1a:GFP*$^{+}$ cells is significantly reduced, 1.8±0.32 cells, in embryos where *etv2* is depleted at 24 hpf by caged MO photoactivation (n=12) (B), compared to uninjected embryos (A) (5.1±0.38 cells, n=13, $p<0.0001$, two tailed student's t-test). Arrows indicate *prox1a:GFP*$^{+}$ endothelial cells. (C) Quantification of *prox1a:GFP* positive cells across the width of 9 somites in the trunk region. Mean±SEM is shown. Individual data points are shown in Fig. S4B. This experiment has been replicated twice.

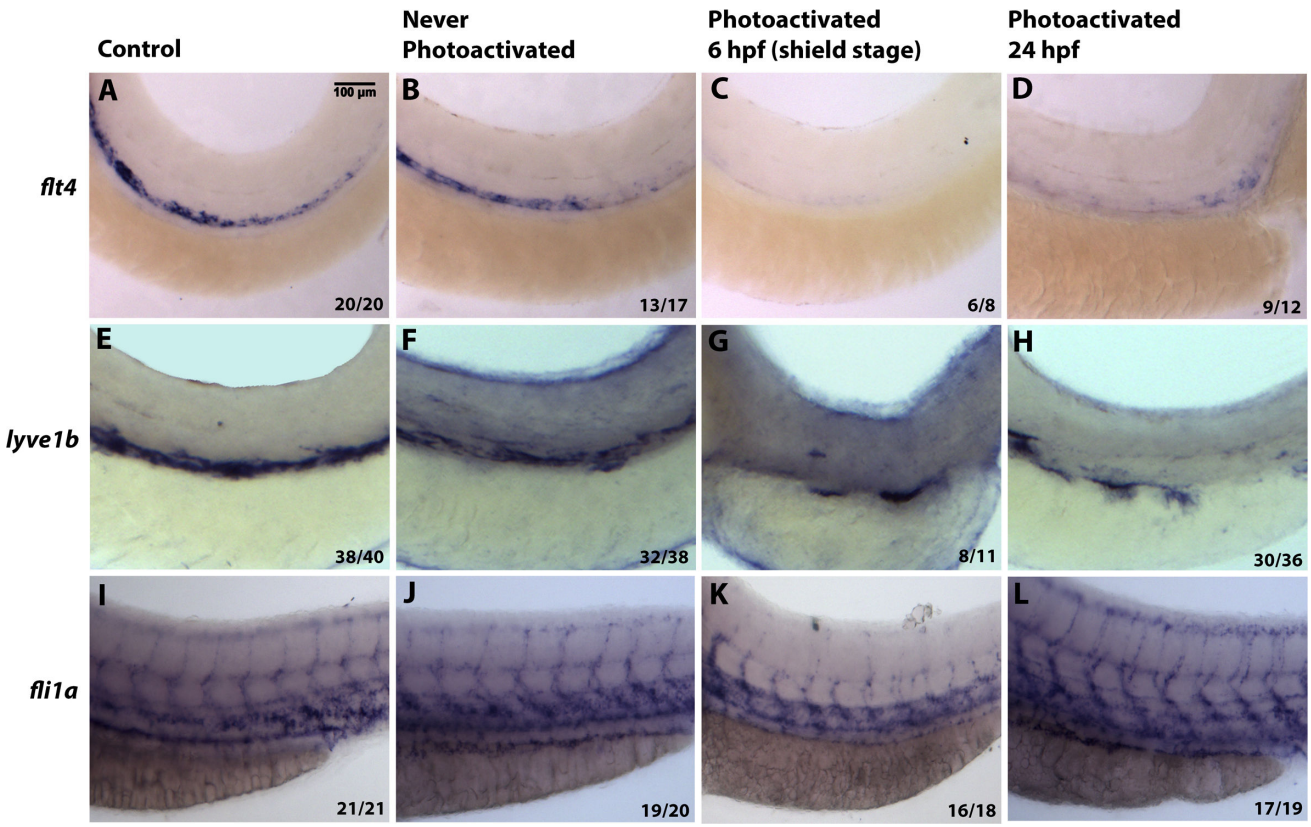

Figure 6. Inducible Etv2 knockdown results in decreased expression of genes associated with lymphangiogenesis as analyzed by *in situ* hybridization at 56 hpf

(A, E, I) Uninjected larvae illustrate normal *flt4, lyve1b* and *fli1a* expression in the PCV. (B, F, J) Larvae injected with photomorph solution and kept in dark show expression pattern similar to uninjected controls. (C, G, K) Larvae injected with photomorph solution and photoactivated at the shield stage (6 hpf) show absent *flt4* and *lyve1b* expression from the major axial vessels. *fli1a* expression is present in the axial vessels due to partial recovery of Etv2 knockdown phenotype observed at the later stages; however, ISV sprouting is abnormal. (D, H, L) Injected larvae photoactivated at 24 hpf, show decreased *flt4* and *lyve1b* expression (D,H), compared to control larvae. However, note the unaffected pattern of *fli1a* (L), demonstrating that Etv2 knockdown at 24 hpf specifically affects markers associated with lymphangiogenesis. Analysis for each marker has been repeated at least twice. Number of larvae showing a displayed phenotype out of the total number of larvae is shown in the lower right corner.

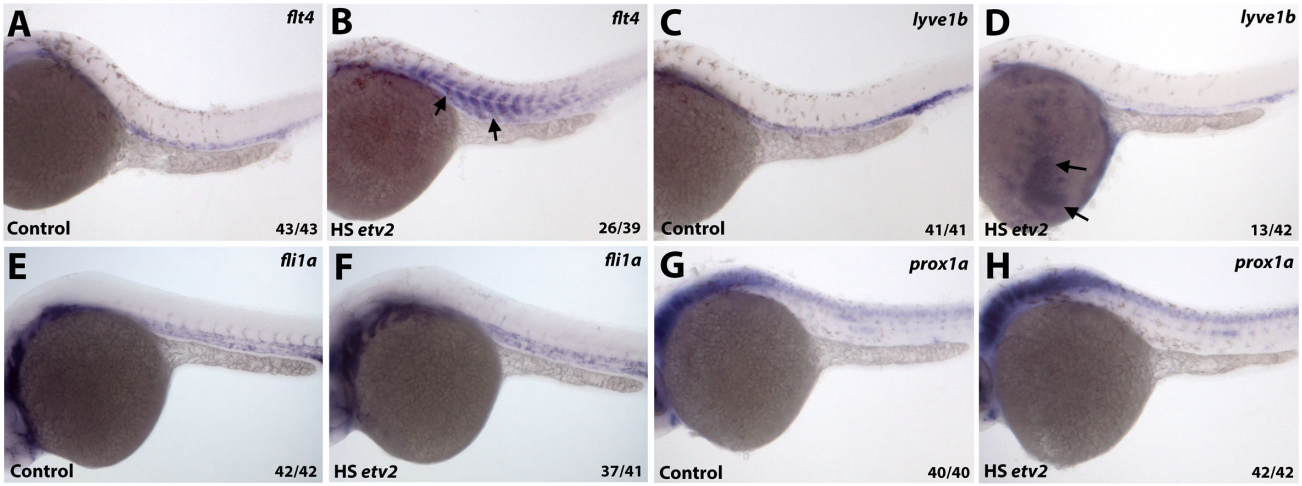

Figure 7. Heatshock inducible overexpression of Etv2 induces ectopic *flt4* and *lyve1b* expression

(A,B) Embryos injected with *hsp70:Etv2-mCherry* overexpression construct show ectopic induction of *flt4* (B) in the somites (arrows) following the heat-shock compared to uninjected controls (A). (C,D) Ectopic expression of *lyve1b* over the yolk is apparent in a subset of embryos that overexpress *hsp70:Etv2-mCherry* (arrows, D). (E–H) No ectopic induction of *fli1a* (E,F) or *prox1a* (G,H) was apparent in the embryos that overexpress *hsp70:Etv2-mCherry*. All embryos are at 28-30 hpf.

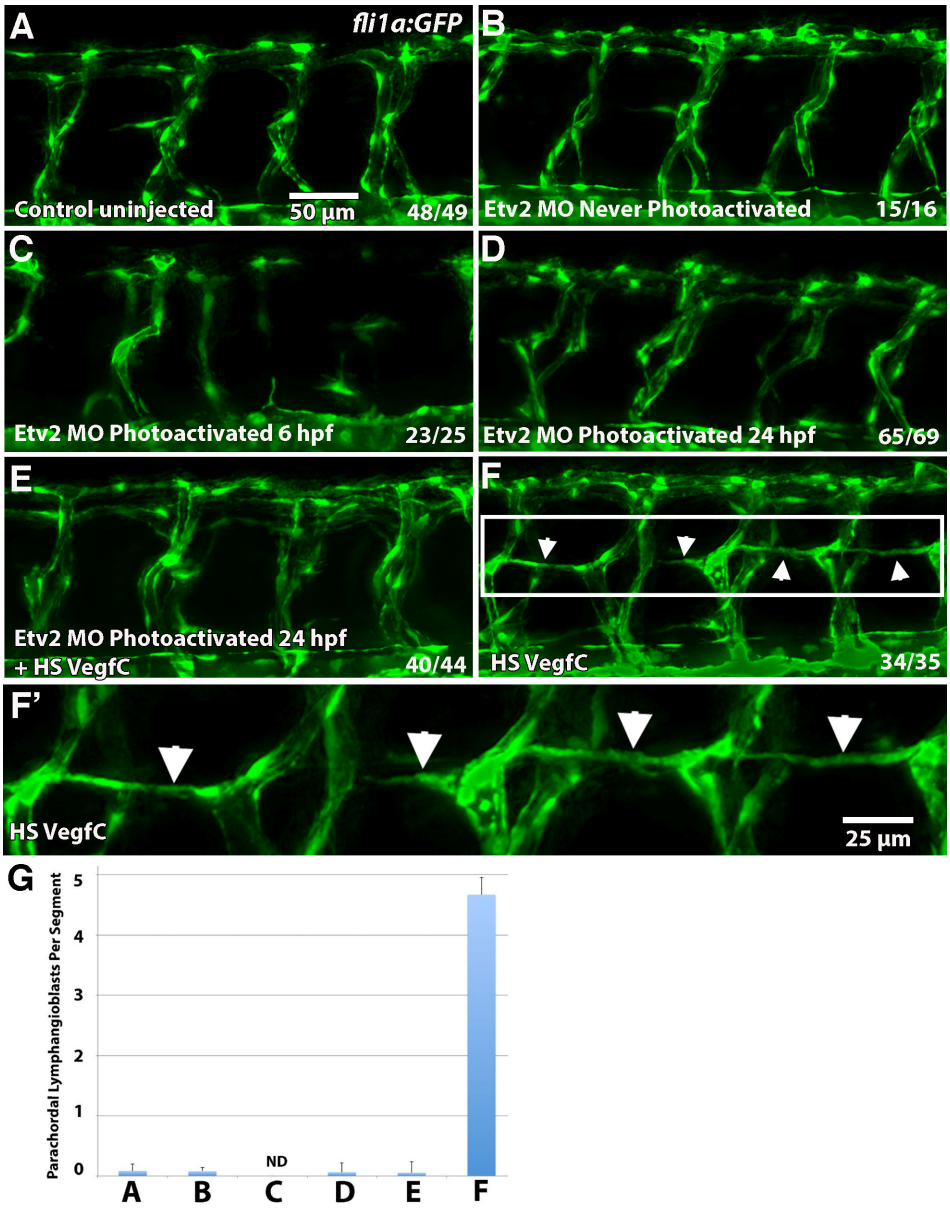

Figure 8. Etv2 function is required for induction of lymphangiogenesis by Vegfc

(A–F) Parachordal lymphangioblasts (PL) were analyzed at 52 hpf in *fli1a:GFP* transgenic line, and visualized by GFP fluorescence, while Etv2 depletion was achieved by UV photoactivation of previously described photomorph solution. (A) Control uninjected larva; (B) Etv2 photomorph injected and never photoactivated larva; (C) Etv2 photomorph injected larva, uncaged at 6 hpf (shield stage); (D) Etv2 photomorph injected larva, uncaged at 24 hpf; (E) Heat-shock Vegfc overexpressing larva, Etv2 depleted by photoactivation at 24 hpf; (F) Larvae injected with heat shock overexpression Vegfc construct only. Note that at this stage there are very few lymphangioblasts in the control larvae (A), while greatly increased number and precocious formation of parachordal lymphangioblasts is observed in Vegfc overexpressing larvae (F, arrows), which are reduced upon Etv2 depletion (C–E). (G) Average number of lymphatic precursor cells per segment. Analysis was accomplished by

counting the number of parachordal lymphangioblasts in ten intersegmental spaces over the trunk of each larva per group. The average number of PLs per segment was then determined. Mean values ± SEM are shown. Note that the larvae were analyzed at 52 hpf, prior to the emergence of PLs in the control group. Larvae that were uncaged at 6 hpf (shield stage) had abnormal vasculature that made calculation of PLs impossible (ND, not determined) (C). The experiment has been replicated twice.

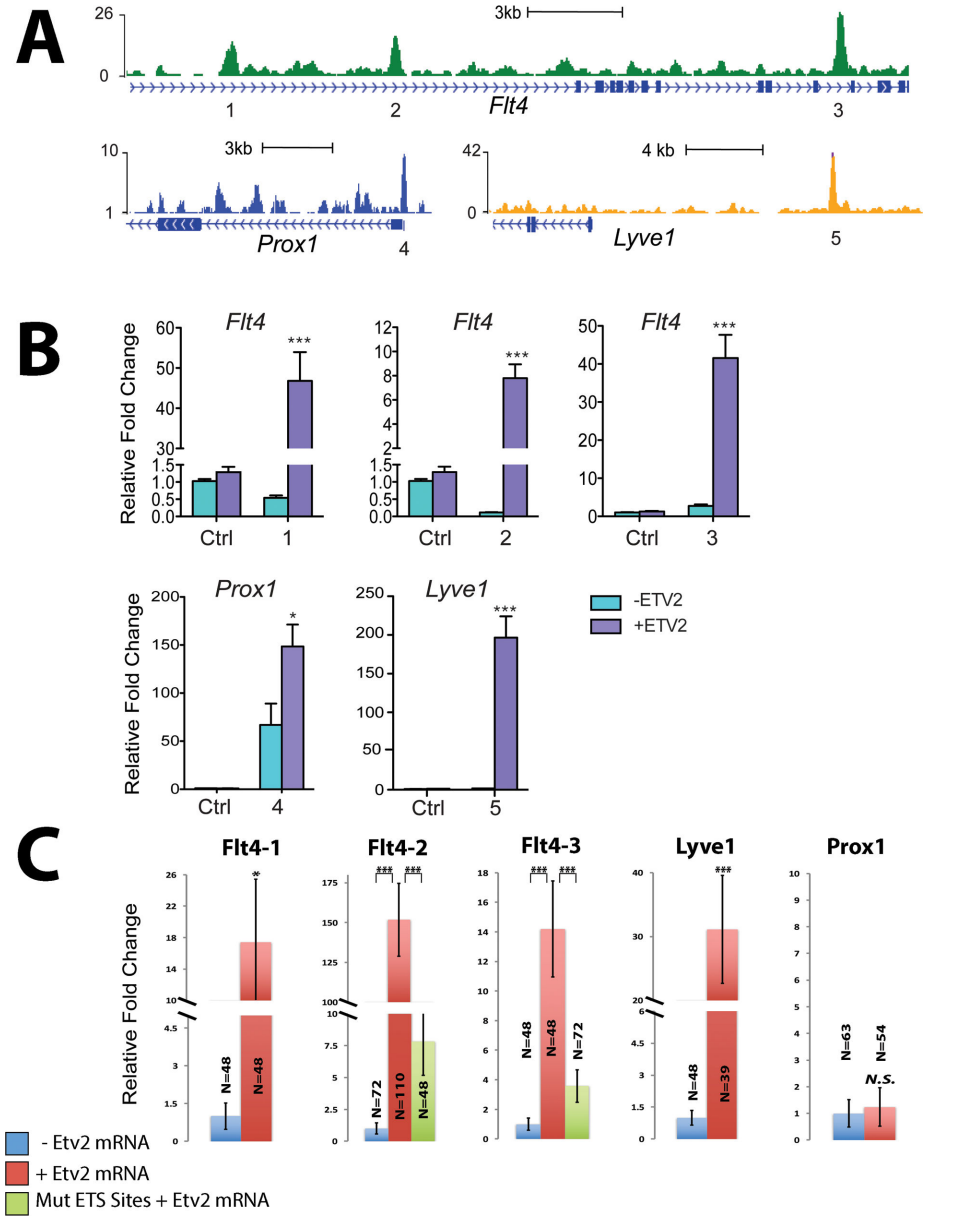

Figure 9. Etv2 directly binds to the promoter / enhancer regions of multiple genes associated with lymphangiogenesis

(A) Genomic snapshots from ChIP-Seq analysis in mouse differentiated ES cells depict the Etv2 binding peaks associated with genes related to lymphangiogenesis. These peak regions denoted by the numbers below (1-5) were further validated by the luciferase reporter assay as shown in (B). Full sequences for each enhancer and consensus ETS binding sites are shown in the Supplemental Table S1. (B) The graph shows relative luciferase activity in 293T cells of each reporter construct containing the Etv2 peak region (1-7) over pGL4.24 control reporter in the presence or absence of murine Etv2 expression plasmids (pMSCV-*Etv2*). Error bars represent the SEM obtained from four biological replicates. Individual data points are shown in Fig. S7. (C) Graphs show relative luciferase activity for each reporter construct as used in (B) injected in zebrafish larvae with or without zebrafish *etv2* mRNA

compared to constructs with mutated ETS binding sites injected along with *etv2* mRNA. * $p<0.05$, *** $p<0.001$, two-tailed Student's t test. Error bars indicate SEM. Individual data points are shown in Fig. S8. Each assay has been replicated at least twice.